Depletion forces in two-dimensional colloidal mixtures

2003 J. Phys.: Condens. Matter 15 S3393

(http://iopscience.iop.org/0953-8984/15/48/001)

INSTITUTE OF PHYSICS PUBLISHING JOURNAL OF PHYSICS: CONDENSED MATTER

J. Phys.: Condens. Matter **15** (2003) S3393–S3409 PII: S0953-8984(03)66581-1

Depletion forces in two-dimensional colloidal mixtures

R Castañeda-Priego, A Rodríguez-López and J M Méndez-Alcaraz

Departamento de Física, Cinvestav, Avenida IPN 2508, Colonia San Pedro Zacatenco, 07360 México DF, Mexico

Received 21 July 2003
Published 20 November 2003
Online at stacks.iop.org/JPhysCM/15/S3393

Abstract

Depletion forces in homogeneous and inhomogeneous binary colloidal mixtures in two dimensions are accounted for by a theoretical approach based on a contraction of the description of liquid mixtures, as well as by computer simulations. We study the depletion interactions in concentrated binary mixtures of additive and non-additive hard discs. The wall–particle depletion potential for a disc close to a hard wall with a concave curvature, or with a relief pattern, is obtained in the infinitely dilute limit, as well as the depletion potentials in mixtures of hard discs and hard plates.

1. Introduction

Colloidal suspensions are present in many inorganic materials, such as paints, glues, inks, etc, and in organic components, such as cells, bacteria, etc. They exhibit interesting transport and structural properties and a great variety of thermodynamic phases, depending on the size, shape and concentration of the constituents. The study of those properties requires a complete understanding of the effective interactions between colloidal particles. Depletion forces are a particular case of these kinds of interactions, which describe the phases of some colloidal systems with an important excluded-volume contribution to the free energy.

Recently, a new theoretical approach for depletion forces, based on the integral equation theory of simple liquids, has been developed, which allows the description of effective interactions in homogeneous and inhomogeneous colloidal suspensions [1, 2]. Basically, it considers the depletion forces as a particular case of the more general effective interactions occurring in a liquid mixture when some species are not considered separately. In the dilute limit this approach contains the well-known Asakura–Oosawa (AO) potential for mixtures of hard spheres [3], which represents the simplest approximation to evaluate the imbalance between the osmotic pressures inside and outside the gap between two colloidal particles approaching each other. Moreover, this theoretical scheme also accounts for general expressions in concentrated systems and captures in a natural way the energetic contributions to the depletion forces when the particles (and/or walls) are interacting through a soft potential (Coulomb, magnetic dipolar, etc).

0953-8984/03/483393+17$30.00

The theoretical formulation mentioned above exploits the covariance property of the Ornstein–Zernike (OZ) equation under contractions of the description. This means, for example, that if only a part of the system or some species can be observed, which can be due to the limitations of the experimental techniques, the OZ equation for the visible particles keeps the same form as the OZ equation for the complete system. The influence of the unobserved particles on the behaviour of the observed ones is captured in an effective pair interaction potential between the latter ones.

In the last few years, effective interactions, static properties and dynamic effects in confined colloidal suspensions have been investigated using quasi-two-dimensional experimental models [4–7]. These systems can be produced by confining the colloids between two plates or by trapping the particles at the interface between two media (e.g. air–water). In this paper we study the entropy-driven forces in perfectly two-dimensional colloidal systems. We believe that our theoretical results could be corroborated with the experimental models mentioned above.

It is known that entropic (or excluded-volume) effects can produce crystal arrays when the colloids are in front of concave walls [8]. Also, the functions of a cell can be affected by the depletion forces between its membrane (wall) and the macromolecules (colloidal particles) within [9, 10]. This means that the geometric features play an important role in the physical properties of such systems. Encouraged by those phenomena, we study the behaviour of the wall–particle depletion potential when the walls have a concave curvature or a relief pattern.

We extend the theory mentioned above to the case of mixtures of spherical and non-spherical colloidal particles. This system is relevant because many biological systems are composed of non-spherical particles, for example a TMV-like virus or fd-bacteriophage. Depletion forces are also present and play an important role in those systems [11]. We study a binary mixture of hard discs and hard plates in the infinitely dilute limit.

This paper is organized as follows. In section 2 we present the general formulation for the effective interaction potentials. In section 3 we study the depletion potentials in dilute and concentrated systems of hard discs by using the theoretical approach mentioned previously, and we also compare our results with data obtained from molecular dynamics (MD) computer simulations. We also investigate the potentials in concentrated binary mixtures of additive and non-additive hard discs. In section 4 we study the wall–particle depletion potential for a hard disc in front of a hard wall with a concave curvature or with a relief pattern. In section 5 we present the results for mixtures of hard discs and hard plates. Here, we also discuss wall effects. The paper ends with a section of conclusions.

2. Effective potentials

2.1. Homogeneous case

The structure of an homogeneous mixture of p spherical species is given by the coupled OZ equations [12]:

$$h_{ij}(r) = c_{ij}(r) + \sum_{k=1}^{p} n_k \int_V c_{ik}(r')h_{kj}(|\mathbf{r} - \mathbf{r}'|)\,\mathrm{d}\mathbf{r}', \tag{1}$$

where $i, j = 1, \ldots, p$. The functions $h_{ij}(r)$ and $c_{ij}(r)$ are the total and direct correlation functions between particles of species i and j, respectively, separated by the distance r. The coefficient n_k is the number density of species k. For the case in which we can only observe the particles of species i, equation (1) takes the one-component form

$$h_{ii}(r) = c_{ii}^{\mathrm{eff}}(r) + n_i \int_V c_{ii}^{\mathrm{eff}}(r')h_{ii}(|\mathbf{r} - \mathbf{r}'|)\,\mathrm{d}\mathbf{r}', \tag{2}$$

where

$$\tilde{c}_{ii}^{\mathrm{eff}}(q) = \tilde{c}_{ii}(q) + \sum_{l\neq i}^{p} \frac{n_l \tilde{c}_{il}(q)\tilde{c}_{li}(q)}{[1 - n_l \tilde{c}_{ll}(q)]} + \sum_{l\neq i}^{p} \sum_{m\neq i\neq l}^{p} \frac{n_l n_m \tilde{c}_{im}(q)\tilde{c}_{ml}(q)\tilde{c}_{li}(q)}{[1 - n_l \tilde{c}_{ll}(q)][1 - n_m \tilde{c}_{mm}(q)]} + \cdots. \tag{3}$$

The function $h_{ii}(r)$ in equation (2) is the same function of equation (1) for the complete system, or original mixture, which does not change after the contraction because the structure of the visible particles remains the same, independent of our ability to distinguish between different components. Equation (3) is written in Fourier space (this feature is indicated by the tilde and by the functional dependence on the wavenumber q) and is a closed equation. The function $c_{ii}^{\mathrm{eff}}(r)$ is the so-called effective direct correlation function [1].

The general form of the effective interaction potential between particles of the observed species is given by the general closure relation for the OZ equation [12]:

$$\beta u_{ii}^{\mathrm{eff}}(r) = \begin{cases} +\infty & r < \sigma_i \\ -c_{ii}^{\mathrm{eff}}(r) + h_{ii}(r) + B_{ii}^{\mathrm{eff}}(r) - \ln[1 + h_{ii}(r)] & r \geqslant \sigma_i. \end{cases} \tag{4}$$

Here, $B_{ii}^{\mathrm{eff}}(r)$ is the effective bridge function and σ_i is the diameter of the particles of species i. In general, the functional form of the bridge function is unknown, but it depends on density so that in very dilute systems its effects are negligible. In that case we can approach equation (4) with

$$\beta u_{ii}^{\mathrm{eff}}(r) = \begin{cases} +\infty & r < \sigma_i \\ -c_{ii}^{\mathrm{eff}}(r) & r \geqslant \sigma_i. \end{cases} \tag{5}$$

Equation (5) is the simplest approximation that we can make for the evaluation of the depletion potentials and corresponds to the mean spherical approximation (MSA) [12]. As we show in the next section, this approximation also works very well for concentrated systems. If we put equation (3) into (5) the effective potential is given by

$$\beta u_{ii}^{\mathrm{eff}}(r) = \begin{cases} +\infty & r < \sigma_i \\ -c_{ii}(r) - \displaystyle\sum_{l=1,l\neq i}^{p} n_l \mathcal{F}^{-1}\left[\frac{\tilde{c}_{il}(q)\tilde{c}_{li}(q)}{1 - n_l \tilde{c}_{ll}(q)}\right] + \cdots & r \geqslant \sigma_i, \end{cases} \tag{6}$$

where $\mathcal{F}^{-1}$ denotes the inverse Fourier transform. In the infinitely dilute limit of the observable species ($n_i \to 0$), up to linear terms in the number densities of the contracted species, equation (6) can be written as

$$\beta u_{ii}^{\mathrm{eff}}(r) = \begin{cases} +\infty & r < \sigma_i \\ -\displaystyle\sum_{l\neq i}^{p} n_l \mathcal{F}^{-1}\{\tilde{c}_{il}^{(0)}(q)\tilde{c}_{li}^{(0)}(q)\} + \cdots & r \geqslant \sigma_i \\ -\displaystyle\sum_{l\neq i}^{p} n_l \int_V c_{il}^{(0)}(|\mathbf{r} - \mathbf{r}'|)c_{li}^{(0)}(r')\,\mathrm{d}\mathbf{r}' + \cdots & r \geqslant \sigma_i, \end{cases} \tag{7}$$

where the convolution theorem for Fourier transforms is used and

$$c_{ij}^{(0)}(r) = \begin{cases} -1 & r < \sigma_{ij} = (\sigma_i + \sigma_j)/2 \\ 0 & r \geqslant \sigma_{ij}. \end{cases} \tag{8}$$

The function $c_{ij}^{(0)}(r)$ is the first term in an expansion of the form $c_{ij}(r) = c_{ij}^{(0)}(r) + n_j c_{ij}^{(1)}(r) + \cdots$ [12]. The integral in equation (7) accounts for the volume V_{exc} of the region in the gap between two particles of species i, separated by the distance r, from which the particles of species $l \neq i$ are excluded due to their simultaneous overlap with both particles of species i. This means that in the infinitely dilute limit the theoretical approach captures the theory of AO

for the depletion forces. Moreover, equation (7) also allows us to evaluate depletion potentials in the dilute limit when an analytical result is not possible to obtain, as we shall show in the next sections.

The evaluation of the effective potential in concentrated systems requires a complete knowledge of the direct correlation functions of the original mixture. Therefore, when we study concentrated systems we numerically solve equation (1) by means of a five-parameter version of the Ng method [13] with Percus–Yevick (PY) or Rogers–Young (RY) closure relations [12, 14]. Proceeding along these lines make sense when the contraction of the description is imposed, for example, by experimental techniques unable to detect all the components. Then, equations (4)–(7) allow for an interpretation of the results in terms of models, including the experimentally invisible species. On the other hand, the approach apparently makes no sense when the goal of the contraction of the description is to simplify the mathematical problem. Fortunately, this is not the case. In addition to the whole lot we can learn about depletion forces by just evaluating $u_{ii}^{\mathrm{eff}}(r)$ in the case in which the complete problem can be solved, we can also find that simple approximations for $c_{ij}(r)$ and $h_{ij}(r)$ could lead to useful expressions for $u_{ii}^{\mathrm{eff}}(r)$. Equation (7), for example, does not require the knowledge of $c_{ij}(r)$ and $h_{ij}(r)$ and it still works fine for some cases in which the contracted particles are really not diluted, as we show in the next sections.

2.2. Inhomogeneous case

The structure of colloidal particles of p spherical species close to a wall is given by the inhomogeneous OZ equation [12]

$$h_{\mathrm{w}i}(\mathbf{r}) = c_{\mathrm{w}i}(\mathbf{r}) + \sum_{j=1}^{p} n_j \int_V c_{ij}(|\mathbf{r}-\mathbf{r}'|) h_{\mathrm{w}i}(\mathbf{r}')\,\mathrm{d}\mathbf{r}', \tag{9}$$

with $i, j = 1, \ldots, p$. The functions $h_{\mathrm{w}i}(\mathbf{r})$ and $c_{\mathrm{w}i}(\mathbf{r})$ are the total and direct correlation functions between the wall and particles of species i, respectively. They depend on the position vector $\mathbf{r}$ because the wall breaks the homogeneity of the particle distribution. The function $c_{ij}(r)$ is the same bulk direct correlation function between particles of species i and j appearing in equation (1). Equation (9) has been used extensively to study the density profile of charged and/or uncharged colloidal particles in front of charged or uncharged flat walls [15].

In the case in which only particles of species i are observed, equation (9) can be rewritten as

$$h_{\mathrm{w}i}(\mathbf{r}) = c_{\mathrm{w}i}^{\mathrm{eff}}(\mathbf{r}) + n_i \int_V c_{ii}^{\mathrm{eff}}(|\mathbf{r}-\mathbf{r}'|) h_{\mathrm{w}i}(\mathbf{r}')\,\mathrm{d}\mathbf{r}' \tag{10}$$

with

$$\tilde{c}_{\mathrm{w}i}^{\mathrm{eff}}(\mathbf{q}) = \tilde{c}_{\mathrm{w}i}(\mathbf{q}) + \sum_{l\neq i}^{p} \frac{n_l \tilde{c}_{il}(q)\tilde{c}_{\mathrm{w}l}(\mathbf{q})}{[1-n_l\tilde{c}_{ll}(q)]} + \sum_{l\neq i}^{p}\sum_{m\neq i\neq l}^{p} \frac{n_l n_m \tilde{c}_{il}(q)\tilde{c}_{lm}(q)\tilde{c}_{\mathrm{w}m}(\mathbf{q})}{[1-n_l\tilde{c}_{ll}(q)][1-n_m\tilde{c}_{mm}(q)]} + \cdots. \tag{11}$$

The function $c_{ii}^{\mathrm{eff}}(r)$ in equation (10) is given by (3). The effective interaction potential between the wall and a particle of species i has the general form [12]

$$\beta\Psi_{\mathrm{w}i}^{\mathrm{eff}}(\mathbf{r}) = \begin{cases} +\infty & x < \sigma_i/2 \\ -c_{\mathrm{w}i}^{\mathrm{eff}}(\mathbf{r}) + h_{\mathrm{w}i}(\mathbf{r}) + B_{\mathrm{w}i}^{\mathrm{eff}}(\mathbf{r}) - \ln[1+h_{\mathrm{w}i}(\mathbf{r})] & x \geqslant \sigma_i/2, \end{cases} \tag{12}$$

where x is the perpendicular distance from the surface of the wall to the centre of the particle. Although we only write $x < \sigma_i/2$ and $x \geqslant \sigma_i/2$ in our equations, which makes sense only for flat walls, these conditions have to be read, in general, as the conditions for overlapping and non-overlapping configurations between the wall and the particle. We assume, as in

the homogeneous case, that MSA is a good approximation for the effective potential. Then, equation (12) becomes

$$\beta\Psi_{wi}^{\text{eff}}(\mathbf{r}) = \begin{cases} +\infty & x < \sigma_i/2 \\ -c_{wi}^{\text{eff}}(\mathbf{r}) & x \geqslant \sigma_i/2. \end{cases} \tag{13}$$

If we substitute equation (11) into (13), the wall–particle depletion potential takes the form

$$\beta\Psi_{wi}^{\text{eff}}(\mathbf{r}) = \begin{cases} +\infty & x < \sigma_i/2 \\ -c_{wi}(\mathbf{r}) - \displaystyle\sum_{l\neq i}^{p} n_l \mathcal{F}^{-1}\left\{\frac{\tilde{c}_{il}(q)\tilde{c}_{wl}(\mathbf{q})}{1-n_l\tilde{c}_{ll}(q)}\right\} + \cdots & x \geqslant \sigma_i/2. \end{cases} \tag{14}$$

This equation has already been used in order to calculate the energetic contributions to the wall–particle depletion potential when the contracted species and/or walls are charged [2].

In the infinitely dilute limit of particles of species i, up to linear terms in the density of the unobserved particles, equation (14) takes the form

$$\beta\Psi_{wi}^{\text{eff}}(\mathbf{r}) = \begin{cases} +\infty & x < \sigma_i/2 \\ -\displaystyle\sum_{l\neq i}^{p} n_l \mathcal{F}^{-1}\{\tilde{c}_{il}^{(0)}(q)\tilde{c}_{wl}^{(0)}(\mathbf{q})\} + \cdots & x \geqslant \sigma_i/2 \\ -\displaystyle\sum_{l\neq i}^{p} n_l \int_V c_{il}^{(0)}(|\mathbf{r}-\mathbf{r}'|)c_{wl}^{(0)}(\mathbf{r}')\,\mathrm{d}\mathbf{r}' + \cdots & x \geqslant \sigma_i/2, \end{cases} \tag{15}$$

where $c_{il}^{(0)}(r)$ and $c_{wi}^{(0)}(\mathbf{r})$ take the values -1 in an overlapping configuration and 0 in a non-overlapping configuration, as in equation (8). In three-dimensional systems we were able to employ equation (15) in order to design surfaces of entropic potentials [16]. We show here some calculations for the two-dimensional case, which refer to lines instead of surfaces of entropic potential.

2.3. Non-spherical particles

Let us consider a system composed of non-spherical colloidal particles of p different species. The structure of such a system is given by the orientation-dependent OZ equation [12]

$$h_{ij}(\mathbf{r}_{12},\mathbf{u}_1,\mathbf{u}_2) = c_{ij}(\mathbf{r}_{12},\mathbf{u}_1,\mathbf{u}_2) + \sum_{l=1}^{p}\frac{n_l}{\Omega}\int_V\int_\Omega \mathrm{d}\mathbf{r}_3\,\mathrm{d}\mathbf{u}_3\,c_{il}(\mathbf{r}_{13},\mathbf{u}_1,\mathbf{u}_3)h_{lj}(\mathbf{r}_{32},\mathbf{u}_3,\mathbf{u}_2), \tag{16}$$

where $i, j = 1,\ldots,p$. The functions $h_{ij}(\mathbf{r}_{12},\mathbf{u}_1,\mathbf{u}_2)$ and $c_{ij}(\mathbf{r}_{12},\mathbf{u}_1,\mathbf{u}_2)$ are the total and direct correlation functions between a particle of species i located at $\mathbf{r}_1$ with an orientational vector $\mathbf{u}_1$ and a particle of species j located at $\mathbf{r}_2$ with an orientational vector $\mathbf{u}_2$, respectively. The total solid angle is given by Ω. Here, we restrict ourselves to binary mixtures of spherical particles (species 1) and non-spherical particles (species 2), so that the orientational coordinates of species 1 can be integrated throughout the contraction of species 2.

In the first step of the contraction procedure equation (16) can be exactly rewritten as

$$\begin{aligned} h_{11}(r_{12}) = {} & \left[c_{11}(r_{12}) + \frac{n_2}{\Omega}\int_V\int_\Omega \mathrm{d}\mathbf{r}_3\,\mathrm{d}\mathbf{u}_3\,c_{12}(\mathbf{r}_{13},\mathbf{u}_3)c_{21}(\mathbf{r}_{32},\mathbf{u}_3)\right] \\ & + n_1\int_V \mathrm{d}\mathbf{r}_4\left[c_{11}(r_{14}) + \frac{n_2}{\Omega}\int_V\int_\Omega \mathrm{d}\mathbf{r}_3\,\mathrm{d}\mathbf{u}_3\,c_{12}(\mathbf{r}_{13},\mathbf{u}_3)c_{21}(\mathbf{r}_{34},\mathbf{u}_3)\right]h_{11}(r_{42}) \\ & + \left(\frac{n_2}{\Omega}\right)^2\int_V\int_\Omega \mathrm{d}\mathbf{r}_3\,\mathrm{d}\mathbf{u}_3\,c_{12}(\mathbf{r}_{13},\mathbf{u}_3)\int_V\int_\Omega \mathrm{d}\mathbf{r}_4\,\mathrm{d}\mathbf{u}_4\,c_{22}(\mathbf{r}_{34},\mathbf{u}_3,\mathbf{u}_4)h_{21}(\mathbf{r}_{42},\mathbf{u}_4). \end{aligned} \tag{17}$$

As in the homogeneous case seen before, further contraction steps lead to

$$h_{11}(r_{12}) = c_{11}^{\text{eff}}(r_{12}) + n_1 \int_V \mathrm{d}\mathbf{r}_3\, c_{11}^{\text{eff}}(r_{13}) h_{11}(r_{32}) \tag{18}$$

with

$$c_{11}^{\text{eff}}(r_{12}) = c_{11}(r_{12}) + \frac{n_2}{\Omega} \int_V \int_\Omega \mathrm{d}\mathbf{r}_3\, \mathrm{d}\mathbf{u}_3\, c_{12}(\mathbf{r}_{13}, \mathbf{u}_3) c_{21}(\mathbf{r}_{32}, \mathbf{u}_3) + \cdots . \tag{19}$$

The only difference between equations (3) and (19), apart from the orientational dependence, is that (3) is written in Fourier space and (19) in real space. Thus, in the case in which we cannot observe the particles of species 2, the effective interaction potential between observed particles in their infinitely dilute limit, up to linear terms in n_2, is given by

$$\beta u_{11}^{\text{eff}}(r_{12}) = \begin{cases} +\infty & r_{12} < \sigma_1 \\ -\dfrac{n_2}{\Omega} \displaystyle\int_V \int_\Omega \mathrm{d}\mathbf{r}_3\, \mathrm{d}\mathbf{u}_3\, c_{12}^{(0)}(\mathbf{r}_{13}, \mathbf{u}_3) c_{21}^{(0)}(\mathbf{r}_{32}, \mathbf{u}_3) & r_{12} \geqslant \sigma_1, \end{cases} \tag{20}$$

where $c_{12}^{(0)}(\mathbf{r}_{13}, \mathbf{u}_3)$ and $c_{21}^{(0)}(\mathbf{r}_{32}, \mathbf{u}_3)$ get the values -1 in an overlapping configuration and 0 in a non-overlapping configuration.

Following the same lines, the wall–particle depletion potential in the case of binary mixtures of hard spheres (species 1) and hard non-spherical particles (species 2) in front of a hard wall is found to be

$$\beta \Psi_{\text{w1}}^{\text{eff}}(\mathbf{r}_1) = \begin{cases} +\infty & x < \sigma_1/2 \\ -\dfrac{n_2}{\Omega} \displaystyle\int_V \int_\Omega \mathrm{d}\mathbf{r}_3\, \mathrm{d}\mathbf{u}_3\, c_{12}^{(0)}(\mathbf{r}_{13}, \mathbf{u}_3) c_{\text{w2}}^{(0)}(\mathbf{r}_3, \mathbf{u}_3) & x \geqslant \sigma_1/2, \end{cases} \tag{21}$$

in the infinitely dilute limit of species 1, up to linear terms in n_2. The variable x and the functions $c_{12}^{(0)}(\mathbf{r}_{13}, \mathbf{u}_3)$ and $c_{\text{w2}}^{(0)}(\mathbf{r}_3, \mathbf{u}_3)$ have the same meaning as in equation (15).

We would like to point out that the contraction of the description provides a general and efficient method to construct effective pair potentials in colloidal suspensions. In the following sections, we use the equations previously obtained in order to evaluate the depletion potentials in homogeneous and inhomogeneous binary mixtures of hard particles in two-dimensional systems.

3. Mixtures of hard discs

In the infinitely dilute limit, the depletion potential between discs of species i, immersed in a suspension of discs j ($\neq i$), can be obtained from the evaluation of equation (7), also using the AO procedure [3]. However, for more complex geometries AO becomes intractable. Nevertheless, equation (7) provides a numerical scheme which can be easily implemented in every case. By constructing a spatial grid around the overlapping region, we can check the simultaneous overlapping condition at every point of the grid. If the condition is fulfilled we add a volume element to the integral in equation (7). In the opposite case, we pass on to the next point of the grid.

Let us consider an asymmetric binary mixture of hard discs of diameters σ_1 and σ_2 ($<\sigma_1$) and surface fractions $\varphi_1 = \pi n_1 \sigma_1^2/4$ and $\varphi_2 = \pi n_2 \sigma_2^2/4$. Then, in the dilute limit, the depletion potential between two large discs takes the form

$$\beta u_{11}^{\text{eff}}(r) = \begin{cases} +\infty & r < \sigma_1 \\ -n_2 \mathcal{F}^{-1}[\tilde{c}_{12}^{(0)}(q) \tilde{c}_{21}^{(0)}(q)] & r \geqslant \sigma_1. \end{cases} \tag{22}$$

The direct correlation function $c_{12}^{(0)}(r)$ describes the overlapping and non-overlapping conditions between particles of species 1 and 2 (see equation (8)). In two dimensions the

Fourier transform of a function $f(r)$ is given by the Fourier–Bessel (FB) transform. Then, the FB transform of $c_{12}^{(0)}(r)$ is

$$\tilde{c}_{12}^{(0)}(q) = 2\pi\sigma_{12}\frac{J_1(q\sigma_{12})}{q}, \tag{23}$$

where $J_n(z)$ is the Bessel function of the first kind of order n. Then, by putting equation (23) into (22), the depletion potential between two large discs takes the form

$$\beta u_{11}^{\text{eff}}(r) = \begin{cases} +\infty & r < \sigma_1 \\ -2\pi\sigma_{12}^2 n_2 \displaystyle\int_0^\infty \frac{J_0(qr)J_1^2(q\sigma_{12})}{q}\,\mathrm{d}q & r \geqslant \sigma_1. \end{cases} \tag{24}$$

The AO procedure, the integral in equation (7) and the numerical evaluation of equation (24) all lead to

$$\beta u_{11}^{\text{eff}}(r) = -\frac{2\varphi_2}{\pi}(1+\eta)^2\left[\cos^{-1}\left(\frac{1}{1+\eta}\frac{r}{\sigma_2}\right) - \left(\frac{1}{1+\eta}\frac{r}{\sigma_2}\right)\sqrt{1-\left(\frac{1}{1+\eta}\frac{r}{\sigma_2}\right)^2}\right] \tag{25}$$

for $\sigma_1 \leqslant r \leqslant \sigma_1 + \sigma_2$ and 0 for larger distances, and $\eta = \sigma_1/\sigma_2$. This potential is always attractive and it has an absolute minimum at contact of amplitude

$$\beta u_{11}^{\text{eff}}(\sigma_1^+) = -\frac{2\varphi_2}{\pi}(1+\eta)^2\left[\cos^{-1}\left(\frac{\eta}{1+\eta}\right) - \left(\frac{\eta}{1+\eta}\right)\sqrt{1-\left(\frac{\eta}{1+\eta}\right)^2}\right]. \tag{26}$$

In practical situations, it should be better to provide simpler expressions for the potential at contact. In that case, equation (26) can be approximately written as $\beta u_{11}^{\text{eff}}(\sigma_1^+) \simeq -(2\varphi_2/\pi)(1.885\,62\eta^{1/2} + 0.659\,96\eta^{-1/2} + \mathcal{O}(\eta^{-3/2}))$. This is a very good approximation for $\eta \geqslant 2$.

In ternary mixtures, the dilute limit of the depletion potential between two hard discs of species 1 and 2, of diameters σ_1 and σ_2 ($<\sigma_1$), immersed in a bath of hard discs of diameter σ_3 ($<\sigma_2$), is given by the contraction of the third species (not shown here). With $n_1 \to 0$ and $n_2 \to 0$, up to linear terms in n_3, this leads to

$$\begin{aligned}\beta u_{12}^{\text{eff}}(r) = &-\frac{\varphi_3}{\pi}(1+\eta_1)^2\left[\cos^{-1}\left(\frac{r_1}{1+\eta_1}\right) - \left(\frac{r_1}{1+\eta_1}\right)\sqrt{1-\left(\frac{r_1}{1+\eta_1}\right)^2}\right] \\ &-\frac{\varphi_3}{\pi}(1+\eta_2)^2\left[\cos^{-1}\left(\frac{r_2}{1+\eta_2}\right) - \left(\frac{r_2}{1+\eta_2}\right)\sqrt{1-\left(\frac{r_2}{1+\eta_2}\right)^2}\right],\end{aligned} \tag{27}$$

for $\sigma_{12} \leqslant r \leqslant \sigma_{12} + \sigma_3$ and 0 for larger distances. Here, $\varphi_3 = \pi n_3\sigma_3^2/4$, $\eta_i = \sigma_i/\sigma_3$, $r_1 = (\sigma_3/4r)[4(r/\sigma_3)^2 + (1+\eta_1)^2 - (1+\eta_2)^2]$, and $r_2 = 2r/\sigma_3 - r_1$. This potential is also purely attractive with an absolute minimum at contact. As expected, in the case for $\sigma_1 = \sigma_2$, equation (27) reduces to (25). In the case that $\sigma_1 \to \infty$, equation (27) corresponds to the wall–particle depletion potential in a binary mixture in front of a flat wall [1]. We can also obtain analytical expressions for more sophisticated systems by simply evaluating equation (7) with the appropriate overlapping conditions. However, in this section we do not report further in that direction. We look instead at concentration effects and at the accuracy of our approximations. We will come back to the dilute limit when we study wall and geometry effects.

In order to check the accuracy of the theory presented in the previous section, we compare the effective potential obtained from equation (6) with MD computer simulations for some binary mixtures of hard discs of diameters σ_1 and σ_2 ($<\sigma_1$) in the infinitely dilute limit of species 1 ($\varphi_1 \to 0$). The simulated entropic forces were obtained by summing the linear

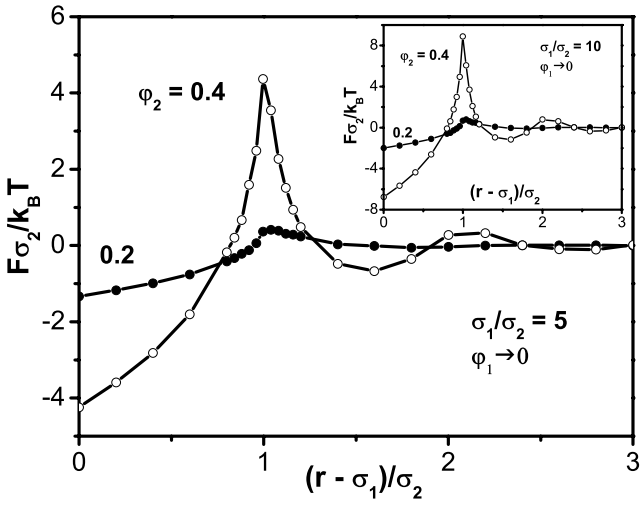

Figure 1. The figure shows the simulated depletion force, scaled with $k_{\mathrm{B}}T/\sigma_2$, between particles of species 1 in two binary mixtures of hard discs with $\sigma_1/\sigma_2 = 5$, $\varphi_1 \to 0$ and $\varphi_2 = 0.2$ and 0.4. The inset also shows the simulated depletion force for the same systems but with $\sigma_1/\sigma_2 = 10$. The curve is just a guide for the eye.

moment exchange over all collisions between all the particles of species 2 and two fixed particles of species 1 separated by a distance r. The depletion potential results from the integration of the force. The computer simulations were performed in a rectangular simulation box with standard periodic boundary conditions, using the Verlet algorithm [17]. The number of particles used in this work for $\sigma_1/\sigma_2 = 5$ was $N_1 = 2$ and $N_2 = 186$ (460) for $\varphi_2 = 0.2$ (0.4). For $\sigma_1/\sigma_2 = 10$ we used $N_1 = 2$ and $N_2 = 408$ (830) for $\varphi_2 = 0.2$ (0.4). The length L of the simulation box was adjusted to give the prescribed density of the system according to the relation $L^2 = N_2/n_2$. At the beginning of the simulation, the two larger hard discs were placed at the centre of the simulation box, separated by a distance r, remaining fixed in that position. The smaller hard discs were then randomly placed in the simulation box in a non-overlapping configuration and allowed to move according to the Verlet algorithm, until equilibrium was reached. Further configurations were generated to calculate the average linear moment exchange. The same procedure was repeated for different values of r in order to achieve the average force over the whole range of significant separations. The average depletion potential results from the integration of the average force. The length L was always large enough for the smaller discs to get their bulk structure on the border of the simulation box. Therefore, the larger particles at the centre of one cell do not sense the other particles of the same species in the other cells.

In figure 1 we can see the simulated effective force between two large hard discs immersed in a bath of small hard discs with surface fractions $\varphi_2 = 0.2$ and 0.4 and size ratios $\eta = 5$. The case with $\eta = 10$ is shown in the inset. The two large discs are placed from the left to the right. The figure shows the amplitude of the force acting on the right disc. A negative value means that this particle feels a force in the direction of the other particle, i.e. an attraction. A positive value means that the particles are repelling each other. We can observe an attractive force when the discs are separated by small distances ($\sigma_1 < r < \sigma_1 + \sigma_2$). This is due to the depletion effect at the AO level. Instead, when they are separated by larger distances there is a repulsive barrier. Basically, this effect is due to the large concentration gradients of small

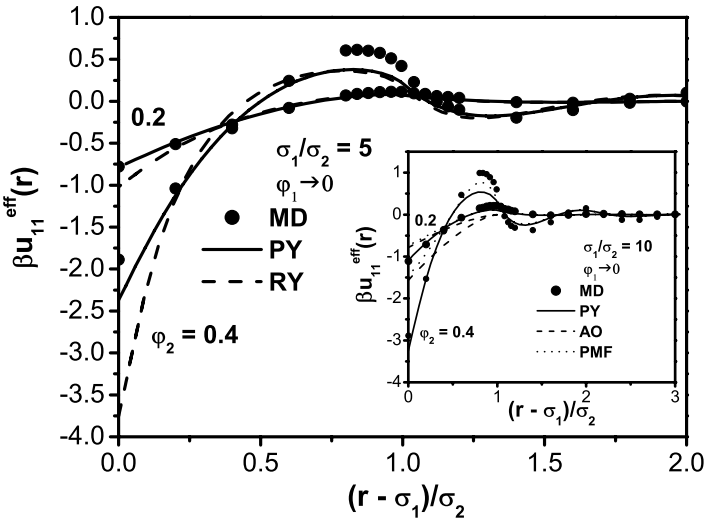

Figure 2. The figure shows the depletion potential $u_{11}^{\mathrm{eff}}(r)$, scaled with $k_{\mathrm{B}}T$, between particles of species 1 in two binary mixtures of hard discs with $\sigma_1/\sigma_2 = 5$, $\varphi_1 \to 0$ and $\varphi_2 = 0.2$ and 0.4. The circles represent the results of the MD simulations. The full curves were obtained from the theoretical approach by solving the OZ equation for the binary mixture with the PY closure relation. The broken curves were obtained with the RY closure relation. The inset shows the depletion potential for the same systems but with $\sigma_1/\sigma_2 = 10$. The broken curves correspond to the AO approximation and the dotted lines stand for the PMF $\beta w_{11}(r) = -\ln g_{11}(r)$.

discs inside and outside the gap between large particles. Both the attractive and repulsive forces mentioned above become stronger with the increasing density of small discs. These features possessed by the effective forces give rise to interesting effects in the behaviour of the depletion potential between large discs, as we see below.

In figure 2 we present the depletion potential for the systems shown in figure 1; $\varphi_2 = 0.2$ and 0.4 and $\eta = 5$. The circles correspond to the MD simulations, and the full and broken lines to the theoretical approach. Here, the correlation functions of the original mixtures were calculated, both with the PY closure relation (full curves) and with the RY closure relation (broken curves). As expected from the results for the force and from the analytical expression for the dilute limit (equation (25)), the attraction at contact becomes deeper as the concentration of small discs increases. At the front of the contact attractive well a repulsive barrier is developed and the interaction becomes more long-ranged, oscillating around 0 for larger distances. This particular behaviour is due to the correlations between small particles, which are not included in the dilute limit, but they are taken into account in the PY and RY approaches. The theory captures all concentration effects with quantitative accuracy. However, we can appreciate that the solution of the OZ equation with the RY closure relation overestimates the amplitude of the potential well at contact, but PY agrees very well with the simulation data. The inset shows the entropic potential for the system $\varphi_2 = 0.2$ and 0.4 and $\eta = 10$. The potential presents basically the same behaviour as the potential with $\eta = 5$, but its main features become more pronounced with increasing asymmetry in size, as expected from equation (25). The potential of mean force (PMF), $\beta w_{11}(r) = -\ln g_{11}(r)$, quantitatively reproduces the potential at large distances. At contact, however, it underestimates the depletion potential as much as the AO approximation does. In the following figures the OZ equation for the original mixture is solved with the PY closure relation.

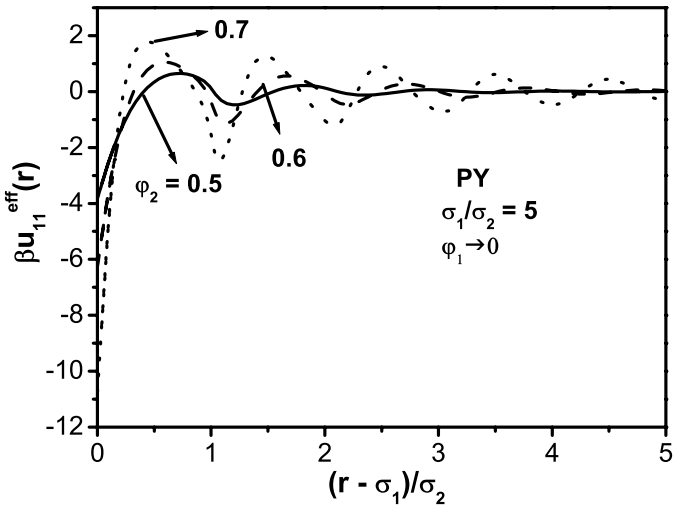

Figure 3. The figure shows the depletion potential $u_{11}^{\mathrm{eff}}(r)$, scaled with $k_{\mathrm{B}}T$, between particles of species 1 in three binary mixtures of hard discs with $\sigma_1/\sigma_2 = 5$, $\varphi_1 \to 0$ and $\varphi_2 = 0.5$, 0.6 and 0.7. The displayed results were obtained from the theoretical approach by solving the OZ equation for the binary mixture with the PY closure relation.

In figure 3 we show the depletion potential between large hard discs immersed in a suspension of small hard discs, in the infinitely dilute limit of the first ones ($\varphi_1 \to 0$) and for large surface fractions of the latter, with a size ratio $\eta = 5$. In this case we observe interesting new effects. For large surface fractions of small hard discs ($\varphi_2 > 0.4$) the position of the first repulsive barrier shifts to smaller distances, until it reaches a new stable position at $r \approx \sigma_1 + \sigma_2/2$. Simultaneously, a new attractive well emerges at $r \approx \sigma_1 + \sigma_2$, where the repulsive barrier was located before. Close to the phase transition ($\varphi_2 = 0.7$) the potential presents strong oscillations around zero at larger distances. This property is characteristic for any system close to the freezing transition, since the correlations between particles become more and more long-ranged when the system approaches the critical point. This behaviour is well captured by the pair depletion potential.

Now, we analyse the effects of increasing the concentration of large discs. In figure 4 we show the depletion potential for a series of systems with $\varphi_2 = 0.3$ and $\eta = 5$, but with different values of φ_1. The potential well at contact becomes deeper with increasing density of large discs. However, this effect is weaker than the effect of increasing the concentration of species 2 shown in figure 3, at least for the present values of φ_1 and φ_2. Also the position of the first barrier shifts to smaller distances and the amplitude of successive wells and barriers increases with φ_1.

A mixture of non-additive hard discs is defined by a non-additive diameter $\sigma_{ij}^{\mathrm{nadd}} = \sigma_{ij} + \Delta_{ij}$, where Δ_{ij} is known as the non-additive parameter. This model has been used as a reference system for mixtures of colloids and polymers, and for mixtures of charged and uncharged particles. Its phase behaviour has been extensively studied as well [18, 19]. Here, we consider binary mixtures of large additive hard discs ($\Delta_{11} = \Delta_{12} = 0$) and small non-additive hard discs ($\Delta_{22} = \Delta \neq 0$) in the infinitely dilute limit of the first ones ($\varphi_1 \to 0$), with a surface fraction $\varphi_2 = 0.2$ of the latter, and a size ratio $\eta = 5$. In figure 5 we show the depletion potential between additive large discs for different values of Δ. For $\Delta = 0$ we recover the additive case already shown in figure 2. When Δ increases the attractive well at

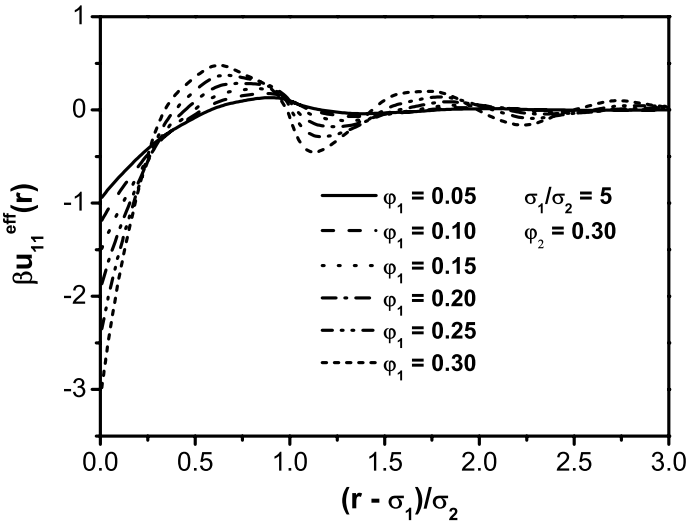

Figure 4. The figure shows the depletion potential $u_{11}^{\mathrm{eff}}(r)$, scaled with $k_{\mathrm{B}}T$, between particles of species 1 in six binary mixtures of hard discs with $\sigma_1/\sigma_2 = 5$, $\varphi_1 = 0.05$, 0.1, 0.15, 0.2, 0.25 and 0.3, and $\varphi_2 = 0.3$. The displayed results were obtained from the theoretical approach by solving the OZ equation for the binary mixture with the PY closure relation.

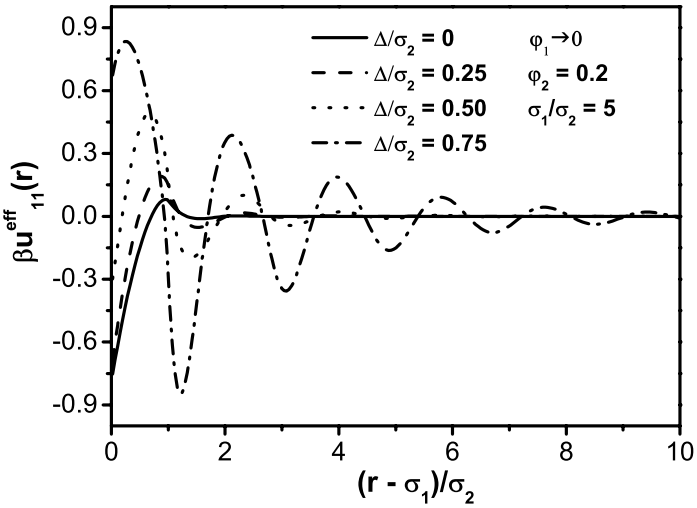

Figure 5. The figure shows the depletion potential $u_{11}^{\mathrm{eff}}(r)$, scaled with $k_{\mathrm{B}}T$, between particles of species 1 in four binary mixtures of non-additive hard discs with $\sigma_1/\sigma_2 = 5$, $\varphi_1 \to 0$, $\varphi_2 = 0.2$, $\Delta_{11} = \Delta_{12} = 0$ and $\Delta_{22}/\sigma_2 = \Delta/\sigma_2 = 0$, 0.25, 0.5 and 0.75. The non-additive diameter is given by $\sigma_{ij}^{\mathrm{nadd}} = \sigma_{ij} + \Delta_{ij}$. The displayed results were obtained from the theoretical approach by solving the OZ equation for the binary mixture with the PY closure relation.

contact disappears, being replaced by a growing repulsive barrier, and the range of the potential increases as well. This result is really amazing, since the same effects are observed when there are energetic contributions to the effective potentials [1, 2]. The non-additive model may allow for the qualitative features of effective potentials in mixtures of hard and soft particles.

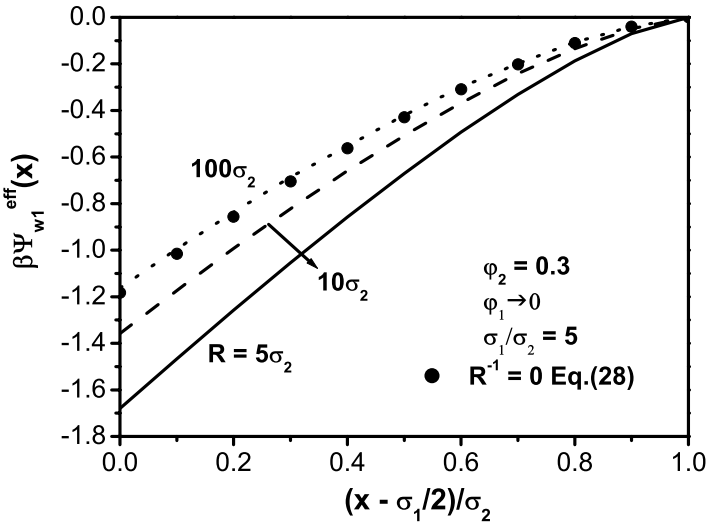

Figure 6. The figure shows the depletion potential $\Psi_{w1}^{eff}(x)$, scaled with k_BT, between particles of species 1 and a two-dimensional hard wall with a concave curvature of radius R in four binary mixtures of hard discs with $\sigma_1/\sigma_2 = 5$, $\varphi_1 \to 0$, up to linear terms in φ_2, and $R/\sigma_2 = 5$, 10, 100 and ∞. The displayed results were obtained from the dilute limit of the theoretical approach. The circles correspond to the case of a flat wall.

4. Wall–particle depletion potentials

We now investigate wall effects. We first consider a binary mixture of large and small discs with diameters σ_1 and σ_2 ($<\sigma_1$) in front of a flat hard wall. The wall–particle depletion potential between the particles of species 1 and the wall in the dilute limit is given by the integration of equation (15) with $p = 2$. It can also be obtained from the limit $\sigma_1 \to \infty$ of equation (27). However, the latter is only useful in the case of flat walls and we shall be focusing on walls with a concave curvature or with a relief pattern. Therefore, in the following we will always work with equation (15). Then, for a flat wall the wall–particle depletion potential is given by

$$\beta\Psi_{w1}^{eff}(x) = -\frac{\varphi_2}{2\pi}(1+\eta)^2\left[\pi + 2\tan^{-1}\left(\frac{1-2x/\sigma_2}{\sqrt{(1+\eta)^2-(1-2x/\sigma_2)^2}}\right)\right] - \frac{\varphi_2}{\pi}(1-2x/\sigma_2)\sqrt{(1+\eta)^2-(1-2x/\sigma_2)^2} \tag{28}$$

for $\sigma_1/2 \leqslant x \leqslant \sigma_1/2 + \sigma_2$ and 0 for larger distances. Here, x is the perpendicular distance from the wall to the centre of the disc of species 1. The depletion potential in equation (28) is only attractive, with an absolute minimum at contact. The wall–particle potential at contact in the inhomogeneous case is more attractive than the potential at contact in the homogeneous case (see equation (27)). This only means that the excluded volume close to a flat wall is larger than that near any other particle of finite diameter.

Now, we consider an asymmetric binary mixture of hard discs in front of a concave hard wall with a radius of curvature R, a surface fraction of small discs $\varphi_2 = 0.3$ and a size ratio $\eta = 5$. We evaluate the potential in the dilute limit by integrating numerically equation (15) with the corresponding overlapping conditions for $c_{12}^{(0)}(r)$ and $c_{w2}^{(0)}(\mathbf{r})$. In figure 6 we show the wall–particle depletion potential for four values of R. The full curves correspond to $R = 5\sigma_2$, the broken curves to $R = 10\sigma_2$, the dotted curves to $R = 100\sigma_2$ and the full circles to $R \to \infty$ or equation (28). When the curvature R^{-1} increases the wall–particle depletion potential at

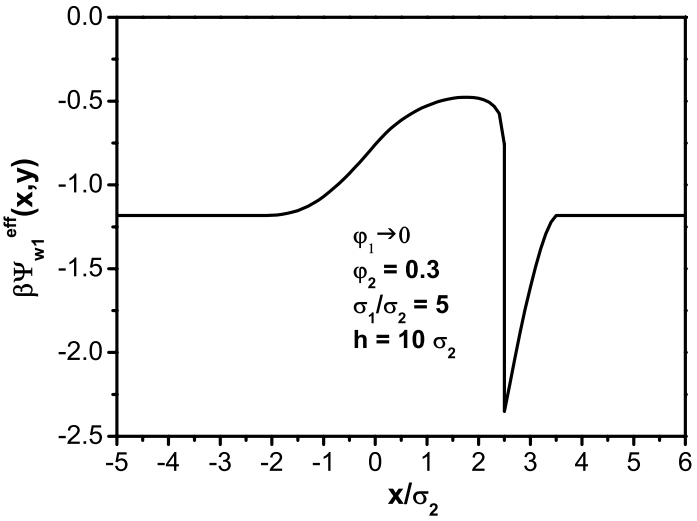

Figure 7. The figure shows the depletion potential $\Psi_{w1}^{\rm eff}(x, y)$ at contact, scaled with $k_{\rm B}T$, between particles of species 1 and a two-dimensional hard wall with a step edge of height $h = 10\sigma_2$, located at $x = 0$, in a binary mixture of hard discs with $\sigma_1/\sigma_2 = 5$ and $\varphi_1 \to 0$, up to linear terms in φ_2. The displayed results were obtained from the dilute limit of the theoretical approach. The curve represents a contact scanning of the wall, beginning on the upper level ($x < 0$) and ending on the lower level ($x > 0$) of the step. The contact value for a flat wall is recovered far away from the step edge.

contact becomes deeper; the larger the curvature the larger the excluded volume. The case of a flat wall is reached in practice when $R \geqslant 100\sigma_2$.

Let us consider now a hard wall with a step edge of height $h = 10\sigma_2$, located at $x = 0$, with the same parameters of the suspension used in the previous case. Here, the variable x has a meaning which differs from the one previously used in this paper. The two-dimensional wall lies along the x axis and the step edge along the y axis. The upper level of the step is in $x < 0$ and the lower level in $x > 0$. In the dilute limit the wall–particle depletion potential is given by the numerical integration of equation (15), with the appropriate overlapping conditions for $c_{12}^{(0)}(r)$ and $c_{w2}^{(0)}(\mathbf{r})$. Figure 7 only shows the contact values of $\beta\Psi_{w1}^{\rm eff}(x, y)$. Thus, the line represents a contact scanning of the wall, beginning on the upper level and ending on the lower level of the step. Closing the edge from the left, the particle first feels a force in the opposite direction, parallel to the wall, and a weaker attraction perpendicular to the wall. Those features arise from the collisions with the small discs in front of the lower level of the step. If the particle is able to cross this barrier, it falls in an attractive well located on the concave edge of the step. Beyond this well the particle only feels a flat wall, as it is always the case far away from the step, in both directions. Some of these predictions have been already observed in the lab [20]. It has also been shown that the attractive well at the concave edge could lead to the selective deposition of particles [8, 21].

In figure 8 we show the contact value of the dilute limit of the wall–particle depletion potential for the same binary mixture of figure 7, but now in front of a hard wall with a barrier of height $h = 10\sigma_2$ and thickness $l = 2\sigma_2$, located at $x = 0$. The top of the barrier is in $-\sigma_2 < x < \sigma_2$. The curve represents therefore a contact scanning of the wall, beginning on one side of the barrier ($x < -\sigma_2$), climbing up, going down and ending on the other side ($x > \sigma_2$). Most of the features of the potential can be understood as a superposition of two opposite lying step edges. However, at the centre of the top of the barrier a second attractive

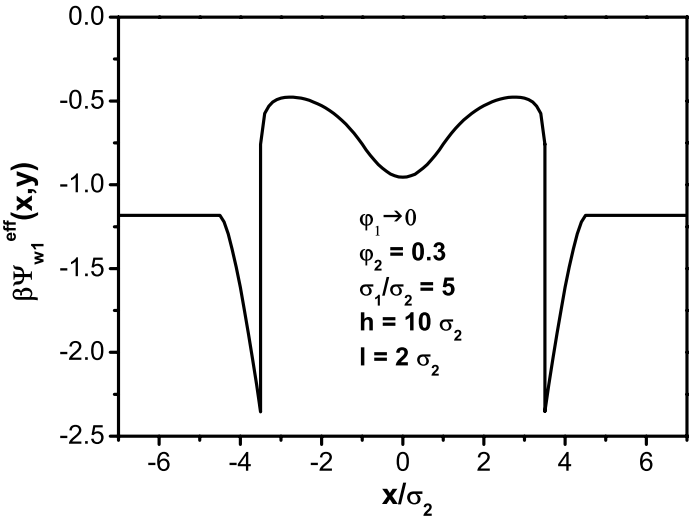

Figure 8. The figure shows the depletion potential $\Psi_{w1}^{eff}(x, y)$ at contact, scaled with $k_B T$, between particles of species 1 and a two-dimensional hard wall with a barrier of height $h = 10\sigma_2$ and thickness $l = 2\sigma_2$, located at $x = 0$, in a binary mixture of hard discs with $\sigma_1/\sigma_2 = 5$ and $\varphi_1 \to 0$, up to linear terms in φ_2. The displayed results were obtained from the dilute limit of the theoretical approach. The curve represents a contact scanning of the wall, beginning on one side of the barrier ($x < -l/2$), climbing up, going down and ending on the other side ($x > l/2$). The contact value for a flat wall is recovered far away from the barrier.

well is developed, which could trap the particle in both directions, parallel and perpendicular to the wall. This could also lead to selective adsorption and has already been used in the synthesis of crystal arrays [21, 22]. We expect that, when $l \geqslant \sigma_1$, the potential well at the top of the barrier reaches its minimum value $\beta\Psi_{w1}^{eff}(x = 0, y = h) = \beta\Psi_{w1}^{eff}(|x| \gg l/2, y = 0)$.

The cases investigated above show that the geometry plays an important role in the behaviour of the wall–particle potential. Equation (15) allows us to design lots of potential profiles by just choosing the geometric features of the wall (or substrate) and/or the parameters of the suspension. Basically, this means that we can handle the entropy of the system. This could be of technological relevance.

5. Binary mixtures of hard discs and hard plates

As mentioned in the introduction many biological systems are composed of non-spherical particles, and depletion forces are also playing an important role in those systems. Encouraged by this fact, we now study mixtures of spherical and non-spherical particles. Such systems have captured the attention of several authors in the past [11, 23]. In the three-dimensional case the depletion potential between spheres immersed in a bath of hard sphero-cylinders displays a quite large contact value compared to $k_B T$. One would expect on this basis to observe a segregation in this kind of mixture. However, such a phase separation has not yet been identified experimentally. That is an example of the open and interesting questions related to such systems.

Several authors have modelled this kind of suspension as two spherical particles (infinitely dilute limit of these species) of diameter σ_1 immersed in a suspension of sphero-cylinders of length L and thickness σ_2, with $\sigma_1 \gg L$ and $L/\sigma_2 \gg 1$. The evaluation of the excluded

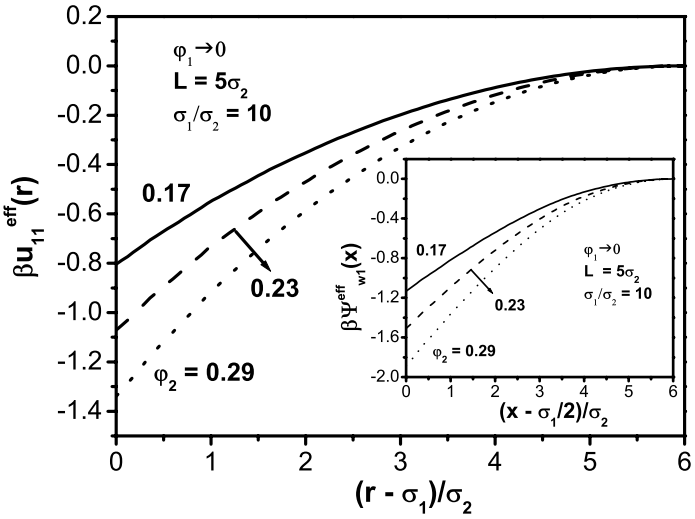

Figure 9. The figure shows the depletion potential $u_{11}^{\rm eff}(r)$, scaled with $k_{\rm B}T$, between particles of species 1 in three binary mixtures of hard discs (species 1) and hard plates (species 2) of thickness σ_2 and length $L = 5\sigma_2$, with $\sigma_1/\sigma_2 = 10$ and $\varphi_1 \to 0$, up to linear terms in φ_2. The displayed results were obtained from the dilute limit of the theoretical approach. Our plates are the two-dimensional equivalent of the sphero-cylinders. The inset shows the depletion potential $\Psi_{\rm w1}^{\rm eff}(x)$, scaled with $k_{\rm B}T$, between particles of species 1 and a two-dimensional flat hard wall in the same three binary mixtures of hard discs (species 1) and hard plates (species 2). The displayed results were also obtained from the dilute limit of the theoretical approach.

volume by using geometrical arguments becomes a tedious problem. Equation (20) allows for a straightforward calculation of the same quantity. We now apply this equation in order to calculate the dilute limit of the depletion potential between hard discs (species 1) of diameter σ_1 immersed in a suspension of hard plates (species 2) of length L and thickness σ_2. Our plates are the two-dimensional equivalent of sphero-cylinders. This means they are rectangular plates of length L and thickness σ_2 ($<L$) ending with half-discs of diameter σ_2. Their surface fraction is then given by $\varphi_2 = (\pi n_2\sigma_2^2/4)(4L/\pi\sigma_2+1)$. We also take $L+\sigma_2 \leqslant \sigma_1$ and values of φ_2 well below the critical density in which two rotating plates partially overlap. When $L = 0$ the case of a binary mixture of hard discs is recovered. Since we are working with two-dimensional systems we have to take $\Omega = 2\pi$ in our equations.

Figure 9 shows the dilute limit of the depletion potential between hard discs of diameter $\sigma_1 = 10\sigma_2$ for three different values of φ_2 and $L = 5\sigma_2$. The depth of the potential well at contact increases with the concentration of plates. $\beta u_{11}^{\rm eff}(r)$ becomes zero when a plate is positioned along the gap between the discs, but not when the plate is perpendicular to the line connecting the centres of the discs. In these systems the potential at contact is more attractive than in the case of asymmetric binary mixtures of hard discs with the same concentration of plates and small discs. The reason for that is related to the fact that the plates possess an additional rotational degree of freedom. Therefore, their entropy is larger than that of small discs.

Figure 10 shows the dilute limit of the depletion potential between hard discs for different lengths of plates. The number partial density of plates has the same value $n_2\sigma_2^2 = 0.05$ in all systems, but φ_2 changes with L. In addition, $\sigma_1 = 10\sigma_2$. The behaviour of the potential is basically the same as in figure 9. However, it is more attractive at contact and more long-ranged when L increases. Also the dilute limit of the wall–particle depletion potential for

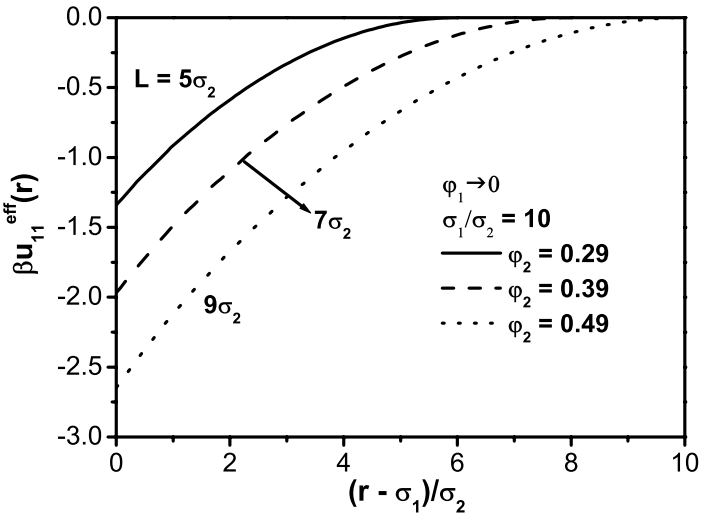

Figure 10. The figure shows the depletion potential $u_{11}^{\mathrm{eff}}(r)$, scaled with $k_{\mathrm{B}}T$, between particles of species 1 in three binary mixtures of hard discs (species 1) and hard plates (species 2) of thickness σ_2 and lengths $L/\sigma_2 = 5$, 7 and 9, with $\sigma_1/\sigma_2 = 10$ and $\varphi_1 \to 0$, up to linear terms in φ_2. The displayed results were obtained from the dilute limit of the theoretical approach. Our plates are the two-dimensional equivalent of the sphero-cylinders.

a hard disc in front of a flat hard wall in a suspension of hard plates is obtained from the numerical evaluation of equation (21). The inset in figure 9 shows this quantity for different values of the concentration of plates. The other parameters are as in the main body of figure 9. The potential at contact becomes deeper with increasing φ_2. The potential well at contact is also deeper than in the homogeneous case. Figures 9 and 10 shall give us a better idea of the applicability of the method.

6. Conclusions

Depletion forces can be understood as a special case of the more general effective interactions arising from the contraction of the description of liquid mixtures. This idea has been implemented within the framework of the integral equation theory of simple liquids [1, 2]. In this paper we apply this theoretical approach in order to evaluate depletion forces in two-dimensional systems. We study dilute and concentrated binary mixtures of hard discs, concentrated binary mixtures of non-additive hard discs and dilute ternary mixtures of hard discs. We also try using inhomogeneous systems, such as dilute binary mixtures of hard discs in front of a hard flat wall, or in front of a hard wall with a concave curvature or with a relief pattern. When working with non-spherical particles, we study dilute binary mixtures of hard discs and hard plates in the bulk and in front of a hard flat wall. In this way, we show that the theory is able to capture concentration and geometrical effects in a natural way. Our results show that the AO [3] approximation is recovered from the dilute limit of our equations, which represents a simple and efficient method to calculate excluded volumes in every geometrical array.

We also calculate the depletion forces by means of MD simulations. The comparison of the simulation data with theoretical results yields an excellent quantitative agreement when the PY approximation is used to calculate the structure of the mixture and the MSA is taken for the effective interaction potential. By working further with these approximations we show that the mixtures of non-additive hard discs may be useful as models for mixtures of hard

and soft particles. The features shown in the depletion forces are very similar to the results obtained from the energetic contributions to the depletion forces in mixtures of charged and uncharged particles [1, 2]. In particular, a salient point is the growth of a repulsive barrier at contact. The systems of additive hard particles behave like the three-dimensional systems. They display a depletion potential well at contact, which is followed, in the case of concentrated systems, by a repulsive barrier. At larger distances, the depletion potential decays, oscillating around zero. More interesting are the results for the wall–particle depletion potential. Our equations allow for the design of potential profiles by just choosing the geometric features of the wall, and/or the parameters of the suspension. Basically, this means that we can handle the entropy of the system. This result could be of technological relevance. On the other hand, the rotational contribution to the entropy of systems composed of non-spherical particles leads to an increment in the amplitude of the depletion attractions.

In our theoretical scheme, depletion forces between two large particles of species 1, immersed in a bath of small particles of species 2, are described as the effective interaction between particles of species 1, mediated by the particles of species 2. Therefore, depletion forces are already a kind of interaction with three-body effects. However, by evaluating the depletion potential we always suppose pairwise additivity of all involved interactions, even the depletion forces themselves. The implementation of triplet interactions in the treatment of the depletion effects constitutes an exciting remaining task.

Acknowledgments

The authors thank CONACyT-Mexico for financial support (grants 33815-E and 0072 'Biomolecular materials'). RCP would like to thank H H von Grünberg and R Klein for useful and interesting discussions and for their hospitality during his stay at the University of Konstanz during the first semester of 2003.

References

[1] Méndez-Alcaraz J M and Klein R 2000 *Phys. Rev.* E **61** 4095
[2] González-Mozuelos P and Méndez-Alcaraz J M 2001 *Phys. Rev.* E **63** 021201
[3] Asakura S and Oosawa F 1964 *J. Chem. Phys.* **22** 1255
[4] Carbajal-Tinoco M D, Castro-Román F and Arauz-Lara J L 1996 *Phys. Rev.* E **53** 3745
[5] Zahn K, Méndez-Alcaraz J M and Maret G 1997 *Phys. Rev. Lett.* **79** 175
[6] Kepler G M and Fraden S 1994 *Phys. Rev. Lett.* **73** 356
[7] Crocker J C and Grier D G 1996 *Phys. Rev. Lett.* **77** 1897
[8] Dinsmore A D and Yodh A G 1998 *Langmuir* **15** 314
[9] Dinsmore A D *et al* 1998 *Phys. Rev. Lett.* **80** 409
[10] Roth R, Götzelmann B and Dietrich S 1999 *Phys. Rev. Lett.* **83** 448
[11] Lin K *et al* 2001 *Phys. Rev. Lett.* **87** 088301
[12] Hansen J P and McDonald I R 1986 *Theory of Simple Liquids* (London: Academic)
[13] Ng K Ch 1974 *J. Chem. Phys.* **61** 2680
[14] Rogers F J and Young D A 1984 *Phys. Rev.* A **30** 999
[15] González-Mozuelos P *et al* 1991 *J. Chem. Phys.* **95** 2006
[16] Castañeda-Priego R, Rodríguez-López A and Méndez-Alcaraz J M 2003 to be submitted
[17] Allen M P and Tildesley D J 1993 *Computer Simulation of Liquids* (Oxford: Science)
[18] Barboy B and Gelbart W M 1979 *J. Chem. Phys.* **71** 3053
[19] Dijkstra M 1998 *Phys. Rev.* E **58** 7523
[20] Dinsmore A D, Yodh A G and Pine D J 1996 *Nature* **383** 239
[21] Castañeda-Priego R 2003 Structure and effective interactions in colloidal suspensions *PhD Thesis* Cinvestav, Mexico
[22] Dinsmore A D 1997 Entropic forces and phase transition in binary nearly hard-sphere colloids *PhD Thesis* University of Pennsylvania
[23] Yaman K, Jeppesen C and Marques C M 1998 *Europhys. Lett.* **42** 221